

Mémoire de Maîtrise en médecine No 2546

Development of blood-brain barrier permeable luciferin analogues for *in vivo* bioluminescent imaging in the brain

Etudiant

Grégoire Michielin

Tuteur

Prof. Elena Dubikovskaya
LCBIM, EPFL

Expert

Dr. Jean-Yves Chatton
DNF, UNIL

Lausanne, Janvier 2016

Résumé

La bioluminescence est un procédé que certaines espèces animales utilisent pour se camoufler, attirer des partenaires ou des proies, ou se défendre contre des prédateurs. Pour émettre de la lumière, une protéine appelée luciférase catalyse l'oxydation d'une petite molécule appelée luciférine. Durant cette réaction, cette molécule est excitée et émet un photon pour retourner à son état fondamental. La bioluminescence est utilisée en biologie dans de nombreuses applications, comme pour détecter l'expression d'un gène, quantifier l'activité d'une enzyme, ou pour étudier le développement de tumeurs. Une des limitations de cette technique est que la luciférine peut difficilement atteindre le cerveau. En effet, le cerveau est protégé par la barrière hémato-encéphalique ou blood-brain barrier (BBB). Ce projet a pour but le développement et l'évaluation de dérivés de la luciférine permettant d'améliorer le passage de cette molécule à travers la BBB.

Notre approche consiste à attacher par estérification un acide gras au groupe hydroxy de la luciférine afin de la rendre plus lipophile. Cette propriété permet à cette nouvelle molécule de passer plus facilement par diffusion à travers la bicouche lipidique. Une fois entrée dans la cellule, la liaison ester est hydrolysée, libérant ainsi la luciférine. Nous avons donc synthétisé et caractérisé une nouvelle classe de dérivés alkylés de D-luciférine et de son précurseur, le 6-hydroxy-2-cyanobenzothiazole (OH-CBT). Ces composés ont été obtenus par estérification avec des acides gras d'une longueur de chaîne de 5 ou 9 carbones, l'acide pentanoïque et l'acide nonanoïque. Les composés correspondants C5-luciférine, C9-luciférine, C5-CBT et C9-CBT ont été obtenus.

Ces nouveaux composés ont montré qu'ils sont de mauvais substrats pour la luciférase en solution, avec pour résultat une faible émission de lumière. En revanche l'hydrolyse de l'acide gras sous l'action d'estérases présentes dans un lysat de cellules permet la libération de la luciférine et ainsi la production de bioluminescence.

La bioluminescence observée *in vitro* dans des cellules exprimant la luciférase est supérieure à la luciférine pour nos composés C5-luciférine et C9-luciférine. Après réaction avec la D-cystéine pour former la luciférine correspondante, le C5-CBT présente également une meilleure bioluminescence que le OH-CBT dont il est dérivé. Nous supposons donc que la plus grande lipophilicité de nos composés alkylés facilite leur diffusion vers l'intérieur des cellules.

Les expériences *in vivo* n'ont pas montré de supériorité des composés alkylés. En effet, l'intensité du signal lumineux émis depuis la région de la tête de la souris n'est pas améliorée par l'utilisation de ces nouvelles molécules. L'utilisation d'une lignée de souris qui exprime la luciférase uniquement dans le cerveau pourrait permettre une meilleure évaluation de l'aptitude des composés à traverser la BBB. Nos molécules présentent toutefois des propriétés nouvelles avec une cinétique de bioluminescence plus lente, ce qui peut être un avantage lors d'expérience nécessitant un temps d'imagerie plus important.

Les prochaines étapes de ce projet consisteront à modifier la D-luciférine et le OH-CBT afin de permettre un transport actif et non passif au travers de la BBB. Il serait possible par exemple d'attacher la D-luciférine à une molécule ou à un peptide transporté de manière active vers le parenchyme cérébral.

Mots-clés: bioluminescence, luciférine, lipophile, blood-brain barrier, *in vivo*

Contents

Résumé	2
Chapter 1 Introduction	4
Chapter 2 Methods	6
2.1 Synthesis	6
2.2 Test tube experiments	6
2.3 <i>In vitro</i> experiments	7
2.4 Formulation for <i>in vivo</i> experiments.....	7
2.5 <i>In vivo</i> experiments.....	7
Chapter 3 Results.....	10
3.1 Test tube experiments	10
3.2 <i>In vitro</i> experiments	13
3.3 <i>In vivo</i> experiments.....	16
Chapter 4 Discussion.....	23
4.1 Synthesis	23
4.2 Test tube experiments	23
4.3 <i>In vitro</i> experiments	24
4.4 Formulation for <i>in vivo</i> experiments.....	26
4.5 <i>In vivo</i> experiments	26
Chapter 5 Conclusion	28
References.....	30

Chapter 1 Introduction

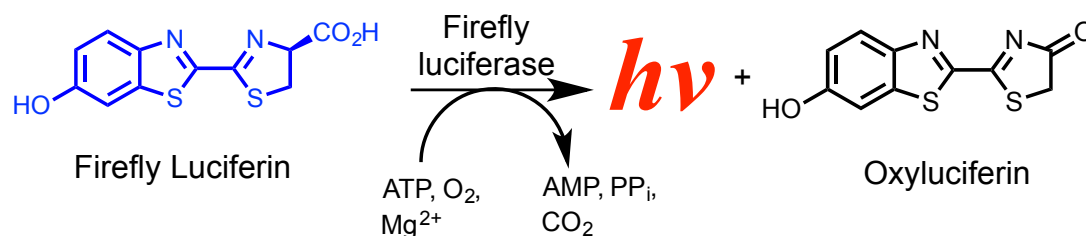


Figure 1-1 Luciferin is oxidized by firefly luciferase in the bioluminescent reaction

Bioluminescence is a biochemical process occurring in nature and used by different species in order to produce light. Enzymes called luciferase are oxidative enzyme that produces bioluminescence upon reaction with their substrates. Firefly luciferase (FLuc) and its substrate, the small molecule D-luciferin, are the most commonly used Luciferase/luciferin pair for *in vivo* bioluminescent imaging (BLI). FLuc uses Mg²⁺, ATP and oxygen to oxidise the D-luciferin into oxyluciferin. As the oxyluciferin produced decays to a lower energy level, it emits a photon with a wavelength around 562 nm (Figure 1-1).

BLI is widely used in biological research as a gene reporter or following tumor growth and cancer cells in living animals. More recently, BLI was used for *in vivo* monitoring of biological processes such as enzymatic activities or metabolites absorption. BLI is of growing interest for live imaging of small animals, as it displays many advantages, such as high signal-to-noise ratio, low cost, ease and safety of use. These characteristics allow for long-term imaging in animals of a particular metabolic process or tumor growth for example, instead of sacrificing the animal at different timepoints. The major drawback is the need for both expression of the luciferase enzyme by the studied organism, and administration of the luciferase substrate, which needs to reach the region of interest in the body of the studied organism(1).

In the study of biological systems, specifically designed chemical reactions are required that are efficient and specific enough to obtain a desired product in physiological conditions, without interfering with biological processes and without reacting with the naturally surrounding organic functions. Chemical reactions that meet these requirements are referred to as bioorthogonal reactions(2).

The condensation between 2-cyano-6-hydroxybenzothiazole (CBT) and L-cysteine (D-Cys) is the naturally occurring reaction in the L-luciferin biosynthesis, which is later converted to D-luciferin(3), and the rate constant for this reaction is very high compared to other bioorthogonal reactions. Based on this observation, a split-luciferin approach has been developed in the group of Elena Dubikovskaya at EPFL (LCBIM) where a click reaction between CBT and D-Cys forms the D-luciferin in a simple and biocompatible way, allowing for protease activity imaging in living mice(4) among other potential applications (Figure 1-2).

Unfortunately, due to their hydrophilic nature, neither D-luciferin nor CBT are able to easily cross the blood-brain barrier (BBB), making *in vivo* BLI in the brain difficult to achieve(5).

Until recently, no published data were available concerning *in vivo* BLI in the brain with unaltered BBB, but some researchers showed that a cyclic alkylated derivative of 6'-amino-luciferin called CycLuc1 displayed a satisfactory BLI signal from the brain using existing luciferase reporters(6). Despite the improvement of the

signal by using this new probe, the luciferase used for brain imaging had to be delivered neurosurgically by stereotactic injection of a viral vector containing an enhanced version of luciferase. As neurosurgical procedures can alter the BBB, development of new probes able to display a high signal in the brain without the need for such procedures is required.

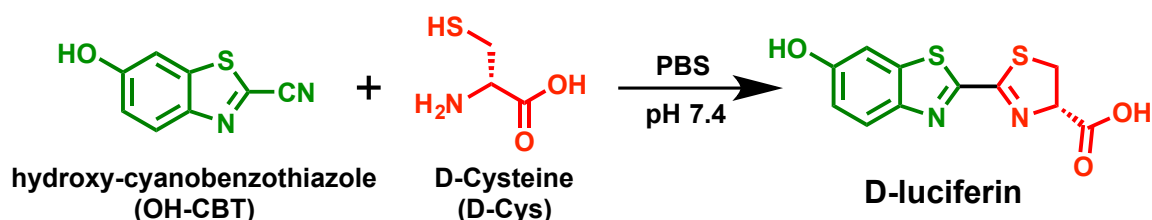


Figure 1-2 Click reaction between hydroxyl-cyanobenzothiazole and D-Cysteine to form D-luciferin in a biocompatible reaction

Among other requirements, a higher lipophilicity is usually linked with an improved passive diffusion across the cell membrane and can therefore help some molecules to access the brain(7). Then, a possible strategy to improve BBB permeability is to add substituents to D-Luciferin and CBT in order to enhance the lipophilicity of these molecules. The approach considered in this project is to form an ester between the 6'-hydroxy group of the D-luciferin and fatty acids of various length, not only making the molecule more lipophilic, but also caging it as it will not be a substrate for luciferase anymore, until the ester bond is hydrolysed and the D-luciferin is released (Figure 1-3).

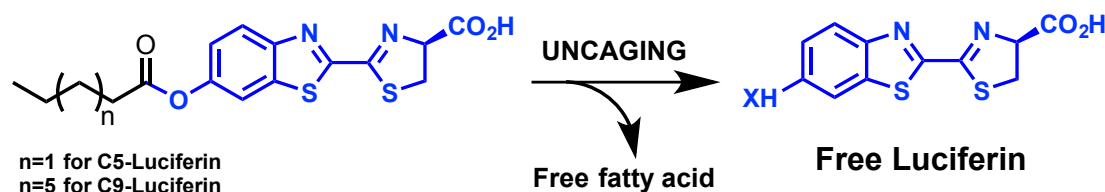


Figure 1-3 Luciferin uncaging upon hydrolysis of the ester bond

In this project, C5-CBT, C9-CBT, C5-Luciferin, C9-Luciferin, C5-Luciferin methyl ester and C9-Luciferin methyl ester (Figure 2-1) were synthesized and evaluated, in a cell-free, cell-based and in living animals experiments. Their potential of bioluminescence as well as their ability to cross the BBB were evaluated in these different environments.

In the light of the promising results recently published for BLI imaging in the brain, continued efforts in the development of novel luciferin derivatives that are able to cross the BBB could open a new field of research to the BLI scientific community and provide some new powerful tools for the neurosciences.

Chapter 2 Methods

2.1 Synthesis

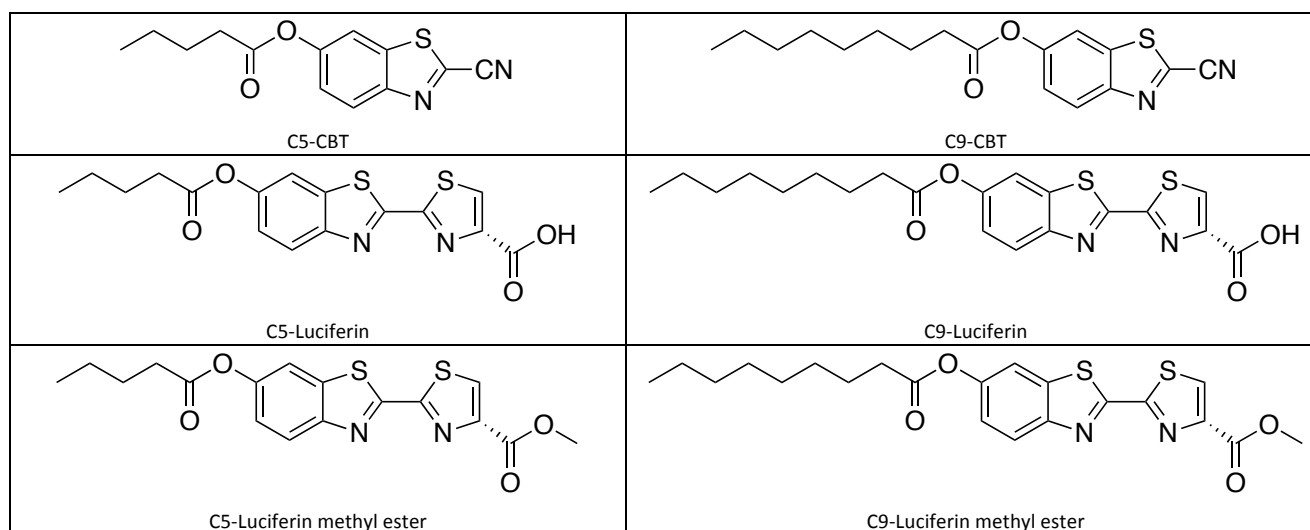


Figure 2-1 Lipophilic derivatives of OH-CBT and D-Luciferin

Lipophilic derivatives of OH-CBT and D-Luciferin were synthesized in the lab. First, an esterification was performed on OH-CBT using pentanoic acid or nonanoic acid to obtain C5-CBT and C9-CBT. In a second step, condensation between the obtained OH-CBT derivatives and D-cysteine or D-cysteine methyl ester yielded C5-Luciferin, C9-Luciferin, C5-Luciferin methyl ester and C9-Luciferin methyl ester. The detailed synthesis description is presented in the section 1.1 of the Annex.

2.2 Test tube experiments

A Perkin Elmer plate reader was used for bioluminescent imaging in the test tube experiments. In a black 96-well plate with clear bottoms (Becton Dickinson and Company) were added 45 μL of luciferase buffer (0,1M Tris-HCl, pH=7.4, 2mM ATP, 5mM MgSO_4) or 45 μL of A549 cell lysate prepared by freeze-thawing A549 cells available in the lab. 5 μL of luciferase (2 $\mu\text{g}/\mu\text{L}$) were added to each well. 50 μL of 100 μM D-cysteine or D-cysteine methyl ester in PBS or 50 μL of PBS alone were added. After 50 μL of 100 μM solution of the different probes were added to the wells, the 96-well plate was immediately placed in the plate reader and imaged for a duration of 150 minutes.

2.3 *In vitro* experiments

This protocol is adapted from Godinat et al(4). IVIS Spectrum Camera (PerkinElmer) was used for bioluminescent imaging in the *in vitro* experiments. 4T1-Luc cells (PerkinElmer) were cultured in RPMI1640 medium obtained from Life Technologies corporation supplemented with 10% FBS and 1% penicillin/streptomycin mixture. Cells were plated (1×10^4 cells/well) in a black 96-well plate with clear bottoms (Becton Dickinson and Company). Then, 48 h after the seeding, the growth medium was removed, and the cells were first washed with 200 μ L of PBS, followed by incubation for 5 min with 100 μ L solution of 100 μ M D-cysteine or D-cysteine methyl ester in PBS for the CBT probes, or PBS alone for the Luciferin probes. After a second addition of 100 μ L solutions of 100 μ M CBT or 100 μ M Luciferin derivatives, the cells were immediately placed in the IVIS Spectrum, and the plate was imaged for a duration of 45 minutes with one image acquired every minute, and reimaged again 45 minutes after the second addition for a duration of 45 minutes. The control compounds were only imaged during this second acquisition.

2.4 Formulation for *in vivo* experiments

The obtained C9-CBT was dissolved in DMSO, PBS, Bovine Serum Albumin (BSA), Tween20, PolyEthylene Glycol (PEG400), Propylene Glycol (PG) or 1,3-propanediol at different concentrations. The obtained C9-Luciferin was dissolved in DMSO, PBS, Bovine Serum Albumin (BSA), PolyEthylene Glycol (PEG400) or Propylene Glycol (PG) at different concentrations. All the resulting solutions were centrifuged for 2 minutes at 6000 rpm to evaluate the solubility.

2.5 *In vivo* experiments

This protocol is adapted from Godinat et al(4). IVIS Spectrum Camera (PerkinElmer) was used for BLI imaging in all animal experiments, and the resulting data were processed using Living Image software (PerkinElmer). All solutions were prepared in sterile DMSO obtained from Sigma-Aldrich and sterile PBS purchased from Life Technologies Corporation. Prior to injection and during the imaging procedure mice were anesthetized by inhalation of isoflurane (Phoenix) that was premixed with oxygen.

2.5.1 Animals

FVB-luc+ (FVB Tg(CAG-luc,-GFP)L2G85Chco/J) transgenic animals mice were purchased from the Jackson Laboratory, and bred at the EPFL (SV-SPF animal facility). The breeding colony was housed in groups of 4–5 mice according to their age and gender with free access to food and water at 22 °C with regular lightdark cycle. All animal experiments were performed according to legislation, using an approved animal license (VD2849). During experiments, 30 to 42 weeks old FVB-Luc+ male were used. Housing was performed in groups of 2–4 mice with free access to food and water at 22 °C with regular lightdark cycle.

2.5.2 Luciferin controls

12 FVB-Luc+ mice were injected intraperitoneally with 0,14 mM D-Luciferin (0,75 mg in 20 μ L DMSO). A solution of D-Luciferin was prepared by dissolving 6,8 mg of D-Luciferin in 181,3 μ L DMSO and injected 20 μ L of solution in the first six mice. A solution of D-Luciferin was again prepared by dissolving 8,92 mg of D-Luciferin in 237,9 μ L DMSO and injected 20 μ L of solution in the next six mice. Right after the injections, mice were anaesthetized and place in the IVIS Specturm imaging chamber under isoflurane anaesthesia. Mice were imaged for 1h with 1 image per minute using the automatic settings.

2.5.3 C5-Luciferin

3 FVB-Luc+ mice were injected intraperitoneally with 0,14 mM C5-Luciferin (0,97 mg in 20 µL DMSO). A solution of C5-Luciferin was prepared by dissolving 7,12 mg of C5-Luciferin in 146,1 µL DMSO and 20 µL of solution were injected in each mice. Right after the injections, mice were anaesthetized and placed in the IVIS Spectrum imaging chamber under isoflurane anaesthesia. Mice were imaged for 1h with 1 image per minute using the automatic settings.

2.5.4 C9-Luciferin

3 FVB-Luc+ mice were injected intraperitoneally with 0,14 mM C5-Luciferin (1,13 mg in 20 µL DMSO). A solution of C9-Luciferin was prepared by dissolving 8,74 mg of C9-Luciferin in 155,3 µL DMSO and 20 µL of solution were injected in each mice. Right after the injections, mice were anaesthetized and placed in the IVIS Spectrum imaging chamber under isoflurane anaesthesia. Mice were imaged for 1h with 1 image per minute using the automatic settings.

2.5.5 OH-CBT controls

12 FVB-Luc+ mice were injected intraperitoneally with 0,14 mM OH-CBT (0,471 mg in 20 µL DMSO) and 0,053 mM D-Cysteine (0,324 mg in 50 µL PBS). A solution of OH-CBT was prepared by dissolving 5,80 mg of OH-CBT in 246,1 µL DMSO and a solution of D-Cysteine by dissolving 5,03 mg of D-Cysteine in 775,8 µL of PBS and 20 µL of the OH-CBT solution were injected in the left part of the intraperitoneal cavity. This was followed by injection of 50 µL of the D-Cysteine solution in the right part of the intraperitoneal cavity of each mice. A solution of OH-CBT was again prepared by dissolving 5,65 mg of OH-CBT in 239,7 µL DMSO and a solution of D-Cysteine by dissolving 6,43 mg of D-Cysteine in 991,8 µL of PBS and 20 µL of the OH-CBT solution were injected in the left part of the intraperitoneal cavity. This was followed by injection of 50 µL of the D-Cysteine solution in the right part of the intraperitoneal cavity of each mice. Right after the injections, mice were anaesthetized and placed in the IVIS Spectrum imaging chamber under isoflurane anaesthesia. Mice were imaged for 1h with 1 image per minute using the automatic settings.

2.5.6 C5-CBT

3 FVB-Luc+ mice were injected intraperitoneally with 0,14 mM C5-CBT (0,696 mg in 20 µL DMSO) and 0.00268 M D-Cysteine (0.324 mg in 50 µL PBS). A solution of C5-CBT was prepared by dissolving 4,51 mg of C5-CBT in 129,6 µL DMSO and a solution of D-Cysteine by dissolving 5,95 mg of D-Cysteine in 918 µL of PBS and 20 µL of the C5-CBT solution were injected in the left part of the intraperitoneal cavity and 50 µL of the D-Cysteine solution in the right part of the intraperitoneal cavity of each mice. Right after the injections, mice were anaesthetized and placed in the IVIS Spectrum imaging chamber under isoflurane anaesthesia. Mice were imaged for 1h with 1 image per minute using the automatic settings.

2.5.7 C9-CBT

3 FVB-Luc+ mice were injected intraperitoneally with 0,14 mM C9-CBT (0,847 mg in 20 µL DMSO) and 0,053 mM D-Cysteine (0.324 mg in 50 µL PBS). A solution of C9-CBT was prepared by dissolving 4,89 mg of C9-CBT in 115,5 µL DMSO and a solution of D-Cysteine by dissolving 5,95 mg of D-Cysteine in 918 µL of PBS and 20 µL of the C5-CBT solution were injected in the left part of the intraperitoneal cavity and 50 µL of the D-Cysteine solution in the right part of the peritoneal cavity of each mice. Right after the injections, mice were anaesthetized and placed in the IVIS Spectrum imaging chamber under isoflurane anaesthesia. Mice were imaged for 1h with 1 image per minute using the automatic settings.

2.5.8 Luciferin controls for tail vein injection

6 FVB-Luc+ mice were injected intravenously with 1,34 mM luciferin (0,085 mg in 200 µL 50%PEG:PG/50%PBS/1%DMSO). A solution of luciferin was prepared by dissolving 3,09 mg of luciferin potassium salt in 36,35 µL DMSO. 6 µL of this solution were diluted in 600 µL PEG:PG 1:1. 500 µL of the resulting solution were diluted in 500 µL PBS and 200 µL were injected in the first three mice. A solution of luciferin was again prepared by dissolving 3,69 mg of luciferin potassium salt in 43,41 µL DMSO. 6 µL of this solution were diluted in 600 µL PEG:PG 1:1. 500 µL of the resulting solution were diluted in 500 µL PBS and 200 µL were injected in the next three mice. Right after the injections, mice were anaesthetized and placed in the IVIS Spectrum imaging chamber under 1% isoflurane anaesthesia. Mice were imaged for 1h with 1 image per minute using the automatic settings.

2.5.9 C5-Luciferin for tail vein injection

3 FVB-Luc+ mice were injected intravenously with 1,34 mM C5-luciferin (equivalent to 0.085 mg luciferin in 200 µL 50%PEG:PG/50%PBS/1%DMSO). A solution of luciferin was prepared by dissolving 3,22 mg of C5-luciferin in 36,03 µL DMSO. 6 µL of this solution were diluted in 600 µL PEG:PG 1:1. 500 µL of the resulting solution were diluted in 500 µL PBS and 200 µL were injected in each mouse. Right after the injections, mice were anaesthetized and placed in the IVIS Spectrum imaging chamber under 1% isoflurane anaesthesia. Mice were imaged for 1h with 1 image per minute using the automatic settings.

2.5.10 C9-Luciferin for tail vein injection

3 FVB-Luc+ mice were injected intravenously with 1,34 mM C9-luciferin (equivalent to 0,085 luciferin mg in 200 µL 50%PEG:PG/50%PBS/1%DMSO). A solution of luciferin was prepared by dissolving 3,85 mg of luciferin potassium salt in 34,22 µL DMSO. 6 µL of this solution were diluted in 600 µL PEG:PG 1:1. 500 µL of the resulting solution were diluted in 500 µL PBS and 200 µL were injected in each mouse. Right after the injections, mice were anaesthetized and placed in the IVIS Spectrum imaging chamber under 1% isoflurane anaesthesia. Mice were imaged for 1h with 1 image per minute using the automatic settings.

Chapter 3 Results

3.1 Test tube experiments

In order to evaluate the potential of our D-Luciferin and OH-CBT for light emission in the presence of firefly luciferase, an experiment in test tubes containing purified luciferase in solution was performed. Luciferase buffer or alternatively A549 cell lysate were added in a black 96-well plate containing luciferase enzyme in all the wells. This was followed by the addition of D-cysteine, D-cysteine methy ester or PBS alone. Finally, the different probes were added to the wells and the 96-well plate was immediately placed in the plate reader and imaged for a duration of 150 minutes. The bioluminescence for controls, C-5 probes and C-9 probes in test tubes containing luciferase alone or with the addition of a cell lysate was obtained and is presented in this section.

3.1.1 Controls

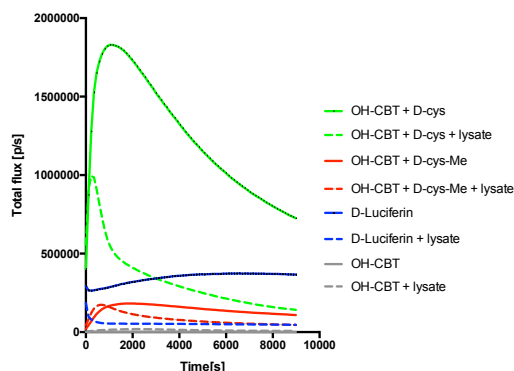


Figure 3-1 Kinetics of light emission for controls in test tubes

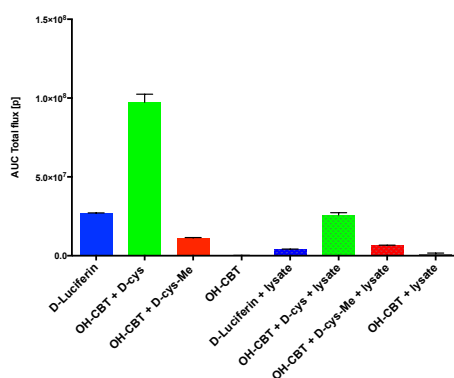


Figure 3-2 Total luminescence for controls in test tubes (150 minutes integration). Error bars are \pm SD for 3 measurements.

The kinetics of light emission for controls in test tubes is presented in Figure 3-1. No peak is observed for D-Luciferin and a plateau in luminescence is observed, whereas OH-CBT shows a strong peak after 20 minutes. After integration of the luminescence over the whole experiment (Figure 3-2), we observe a stronger luminescence for OH-CBT and D-cysteine compared to D-luciferin, while no significant signal is observed from OH-CBT alone. The signal from OH-CBT and D-cysteine methyl ester was lower than the signal for D-cysteine. We noted an influence of the presence of the cell lysate with a global diminution of the observed signal, with an exception for OH-CBT alone where the signal is increased, probably due to the presence of cysteine in the cell lysate.

3.1.2 C5 probes

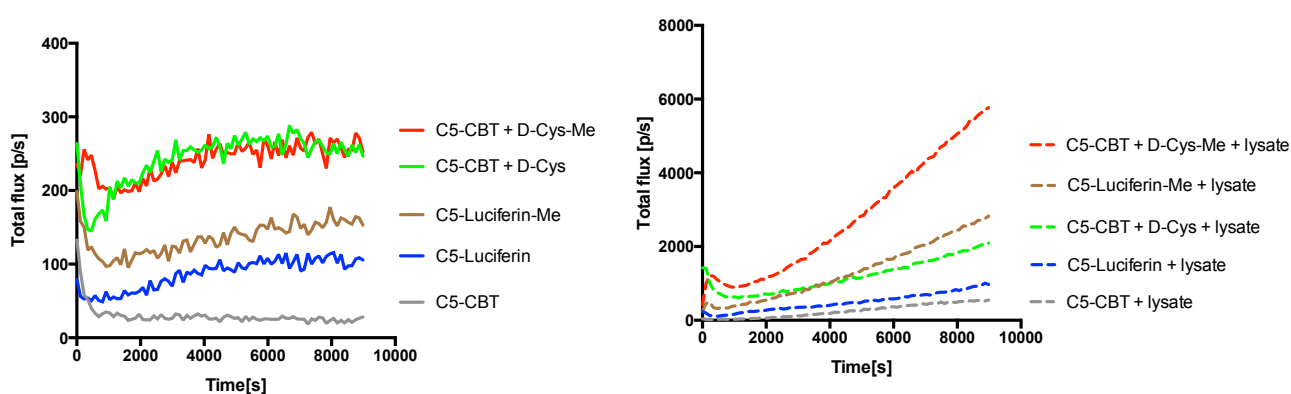


Figure 3-3 Kinetics of light emission for C5 probes in test tubes

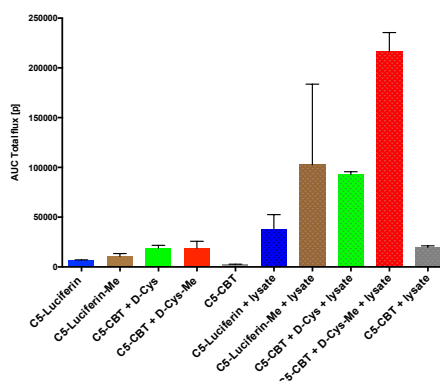


Figure 3-4 Total luminescence for C5 probes in test tubes (150 minutes integration). Error bars are \pm SD for 3 measurements.

The kinetics of light emission for C5 probes in test tubes is presented in Figure 3-3. A very low luminescence is observed when no cell lysate is added to the luciferase solution, suggesting that the C5-probes are not a good substrate of luciferase. Upon addition of cell lysate, the signal increases more than 10-fold over the timecourse of the experiment (150 minutes). After integration of the luminescence over the whole experiment (Figure 3-4), we see a clear effect of the cell lysate in the improvement of the signal. The presence of the methyl ester of cysteine leads to a stronger signal in this experiment.

3.1.3 C9 probes

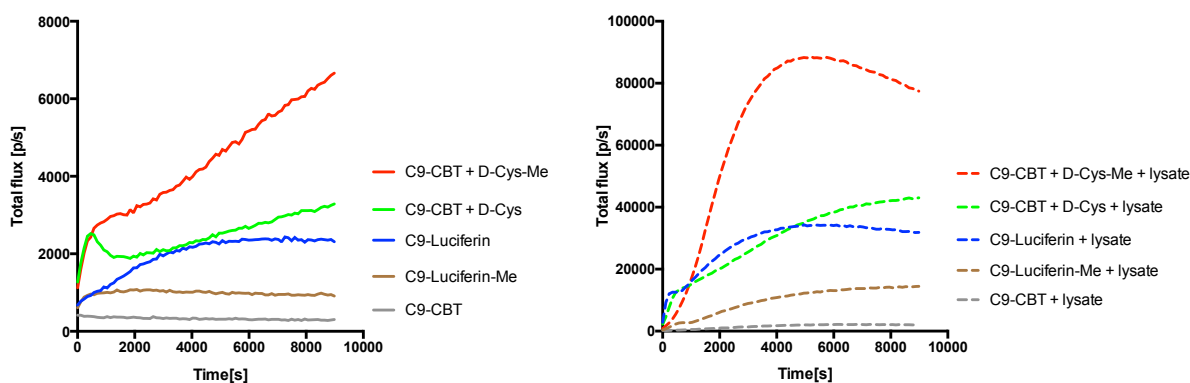


Figure 3-5 Kinetics of light emission for C9 probes in test tubes

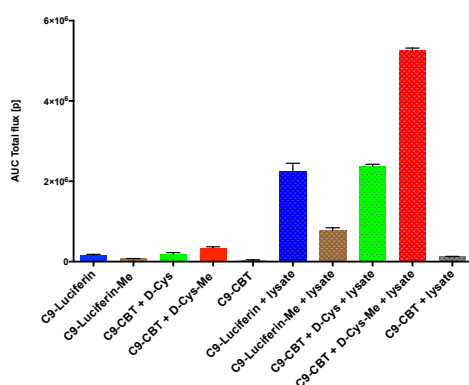


Figure 3-6 Total luminescence for C9 probes in test tubes (150 minutes integration). Error bars are \pm SD for 3 measurements.

The kinetics of light emission in test tubes for C9 probes is presented in Figure 3-5. A very low luminescence is observed when no cell lysate is added to the luciferase solution, suggesting that the C5-probes are not a good substrate of luciferase. However, an increase in the signal seems to occur even in the absence of the cell lysate, indicating a possible hydrolysis of a small fraction of the probes in solution. Upon addition of cell lysate, the signal increases more than 10-fold over the timecourse of the experiment (150 minutes). After integration of the luminescence over the whole experiment (Figure 3-6), we see a clear effect of the cell lysate in the improvement of the signal. In this experiment, the presences of the methyl ester lead to a stronger signal only in combination with the C9-CBT, but not with the already formed C9-luciferin methyl ester.

3.2 *In vitro* experiments

In order to evaluate the bioluminescent potential for our compounds in a cellular environment, *in vitro* experiments were conducted. Cells were plated in a black 96-well plate and incubated with a solution of D-cysteine or D-cysteine methyl ester in PBS (for the CBT probes), or alternatively with PBS alone (for the Luciferin probes). After addition of a solution of CBT or Luciferin derivatives, the cells were immediately placed in the IVIS Spectrum, and the plate was imaged for a duration of 45 minutes with one image acquired every minute, and reimaged again 45 minutes later for another 45 minutes. The bioluminescence for controls, C-5 probes and C-9 probes in 4D1 luciferase transfected cells *in vitro* was obtained and is presented in this section.

3.2.1 Controls

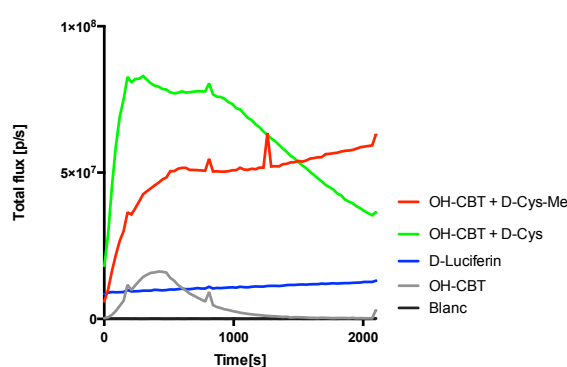


Figure 3-7 Kinetics of light emission for controls *in vitro*

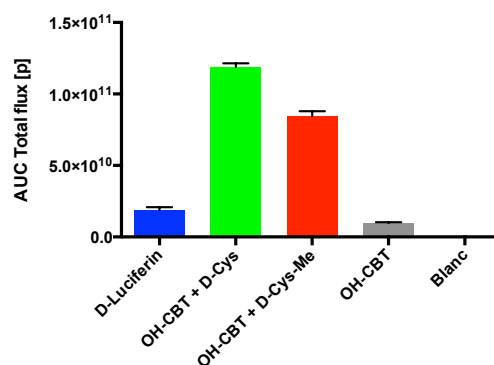


Figure 3-8 Total luminescence for controls *in vitro* (first 30 minutes integration). Error bars are \pm SD for 3 measurements.

The kinetics of light emission *in vitro* for controls is presented in Figure 3-7. Similar to the previous experiment in test tubes, no peak is observed for D-Luciferin and a plateau in luminescence is observed. A stronger signal is observed for OH-CBT combined with D-cysteine or D-cysteine methyl ester than for D-luciferin. A significant signal is present when OH-CBT alone is added to the cells, probably due to the presence of L-cysteine in the cells. After integration of the luminescence over the whole experiment (Figure 3-8), we see a much stronger signal for the split luciferin controls and an advantage of D-cysteine over its methyl ester analog. However, there appears to be a more stable signal for the latter, with a plateau in the bioluminescence that is present even after 30 minutes of imaging.

3.2.2 C5 probes

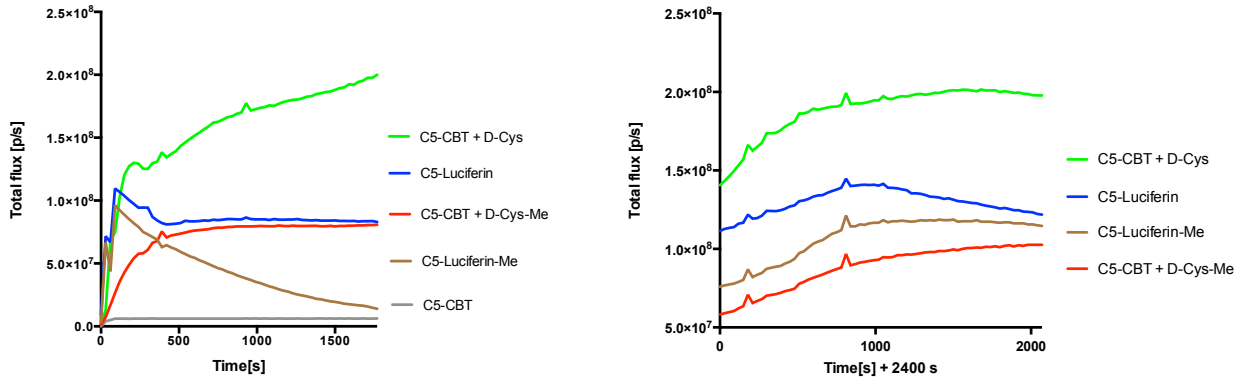


Figure 3-9 Kinetics of light emission for C5 probes *in vitro*

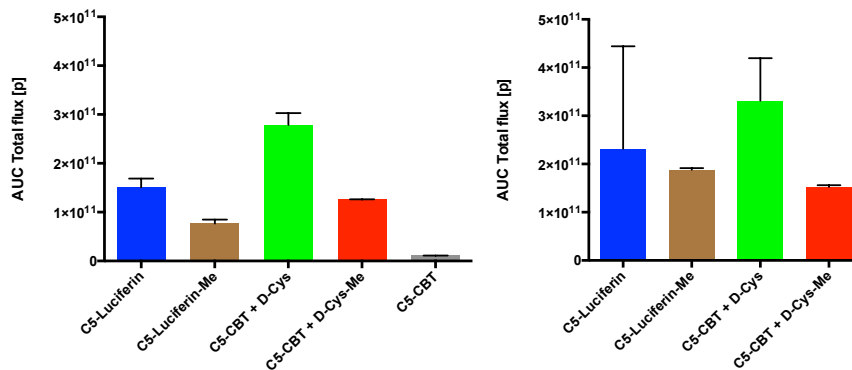


Figure 3-10 Total luminescence for C5 probes *in vitro* (left: first 30 minutes integration, right: minute 40 to 70 integration) . Error bars are \pm SD for 3 measurements.

The kinetics of light emission *in vitro* for C5-probes is presented in Figure 3-9. The panel on the right was obtained by measuring the luminescence 40 minutes after the beginning of the experiment. The C5-CBT combined with D-cysteine presents the strongest rise in bioluminescence, appears to reach a plateau between 1.0×10^8 and 2.0×10^8 *photon/s* after more than 45 minutes and remains higher than the other C5-probes throughout the experiment. Combining C5-CBT with D-cysteine methyl ester results in a slower rise in luminescence and a luminescence two times smaller than D-cysteine once the plateau is reached. C5-luciferin also displays a strong rise in signal and it rapidly stabilises around 1.0×10^8 *photon/s*. The C5-luciferin methyl ester presents a more complicated kinetic with a rapid rise peaking after a few minutes, followed by a decrease in the luminescence, and another rise in signal to reach similar levels as C5-luciferin at the end of the experiment. After integration of the luminescence over the whole experiment (Figure 3-10), we see that the strongest signal comes from C5-CBT combined with D-cysteine having a total light emission two to three times bigger than other C5 probes. We observe that the presence of the methyl ester decreases light emission in luciferase expressing cells. Finally, we note that the *in vitro* luminescence for C5-probes appears to be higher than for controls.

3.2.3 C9 probes

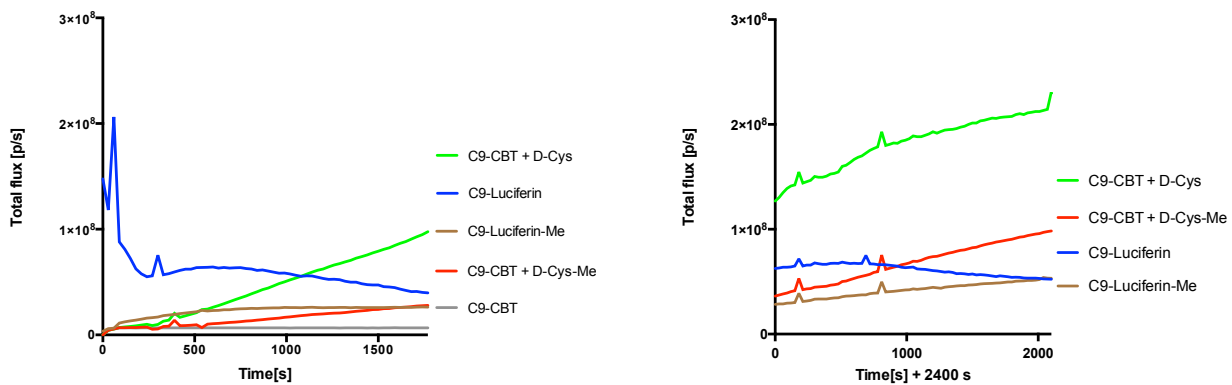


Figure 3-11 Kinetics of light emission for C9 probes *in vitro*

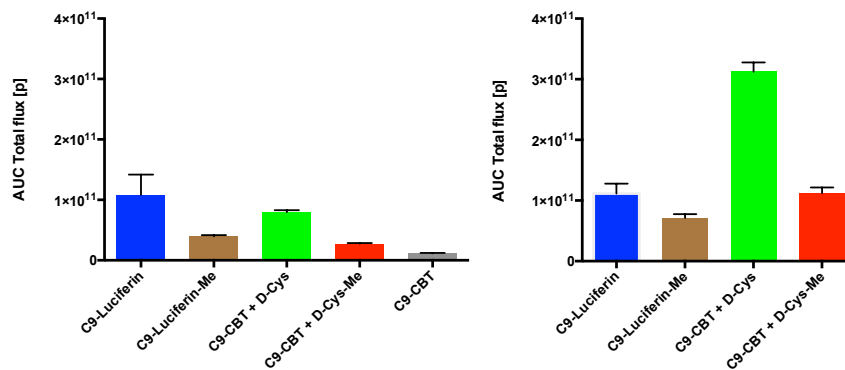


Figure 3-12 Total luminescence for C9 probes *in vitro* (left: first 30 minutes integration, right: minute 40 to 70 integration) . Error bars are \pm SD for 3 measurements.

The kinetics of light emission *in vitro* for C9-probes is presented in Figure 3-11. The panel on the right was obtained by measuring the luminescence 40 minutes after the beginning of the experiment. The C9-CBT combined with D-cysteine presents a slower rise in bioluminescence compared to what was observed for C5-CBT, but reaches the same levels of luminescence between 1.0×10^8 and 2.0×10^8 *photon/s* after more than 45 minutes and the signal seems to keep increasing at the end of the experiment. Similar to our previous observation with C5-CBT, combining C9-CBT with D-cysteine methyl ester results in a slower rise in luminescence and a luminescence two times smaller than D-cysteine once the plateau is reached. C9-luciferin displays a strong rise in signal and it stabilises between 5.0×10^7 and 1.0×10^8 *photon/s*. The C9-luciferin methyl ester luminescence slowly rises and stabilises around 2.5×10^7 . After integration of the luminescence over the whole experiment (Figure 3-12), we see that the strongest signal comes from C9-luciferin in the first 30 minutes of the experiment, but C9-CBT combined with D-cysteine displays a higher total luminescence if we consider the end of the experiment. Again, we observe that the presence of the methyl ester decreases light emission in luciferase expressing cells. Finally, we note that the *in vitro* luminescence for C9-probes appears to be higher than for controls, but a little smaller compared to C5-probes.

3.3 *In vivo* experiments

Our compounds were evaluated for *in vivo* applications in this section. A solution of D-Luciferin, OH-CBT, or their alkylated derivatives was prepared by dissolving the probe in DMSO, and 20 μL of solution were injected intraperitoneally in FVB-Luc+, luciferase-expressing mice. Different formulations were explored to find the least harmful vehicle, while allowing all the compounds to be injected with same formulation for comparison. The high lipophilicity of our compounds made it impossible to solubilize all of them in PBS, BSA, Tween20, PEG400, PG or 1,3-propanediol in various combinations. A small volume of DMSO was the only vehicle in which all the probes could be dissolved and was compatible with *in vivo* injection (see details in Section 1.2 of the Annex). Right after the injections, mice were anaesthetized and placed in the IVIS Spectrum imaging chamber under isoflurane anaesthesia. Mice were imaged for 1h with 1 image per minute using the automatic settings.

3.3.1 D-luciferin controls

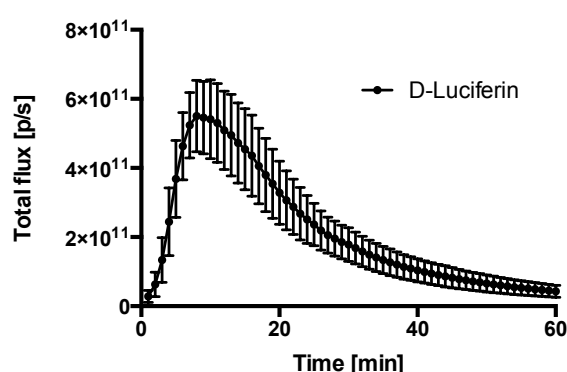


Figure 3-13 Kinetics of light emission for intraperitoneal injection of D-Luciferin *in vivo*. Error bars are \pm SD for 4 measurements.

The kinetics of light emission *in vivo* after intraperitoneal injection of D-luciferin is shown in Figure 3-13. Two mice presented a much lower light emission (Mice 09 and 12, see supplementary figure in the Annex) and were excluded to produce this graph. A strong peak is observed after 10 minutes of imaging followed by a gradual decrease in bioluminescence over the timecourse of the experiment.

3.3.2 Luciferin probes

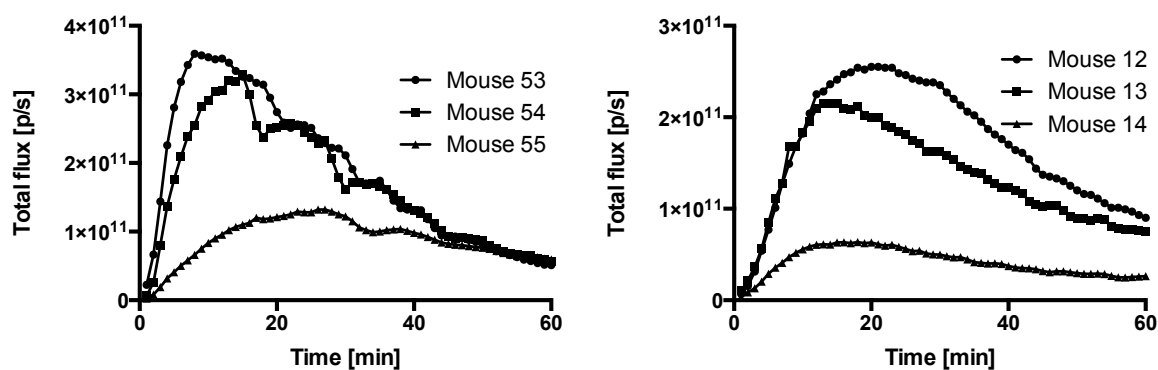


Figure 3-14 Kinetics of light emission for i.p. injection of C5-Luciferin (left) and C9-Luciferin (right) *in vivo*

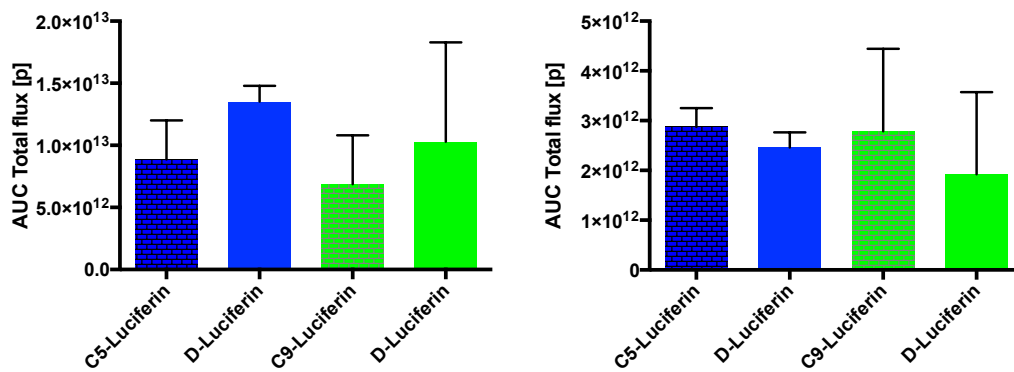


Figure 3-15 Total luminescence for luciferin probes *in vivo* (left: 60 minutes integration, right minute 30 to 60 integration) Error bars are \pm SD for 3 measurements.

The kinetics of light emission *in vivo* after intraperitoneal injection of C5-luciferin and C9-luciferin is presented in Figure 3-14. There is a peak in light emission between 10 and 15 minutes for C5-luciferin, similar to D-luciferin, whereas the peak for C9-luciferin appears later at around 20 minutes. The decrease in light emission appears slower for C5-luciferin and C9-luciferin. The integration over the whole experiment shows no significant difference in the light emission, but there is a trend for a stronger light emission for D-luciferin compared to the probes, but stronger signal for C5 and C9 probes if we consider only the last 30 minutes of imaging only (Figure 3-15).

3.3.3 OH-CBT controls

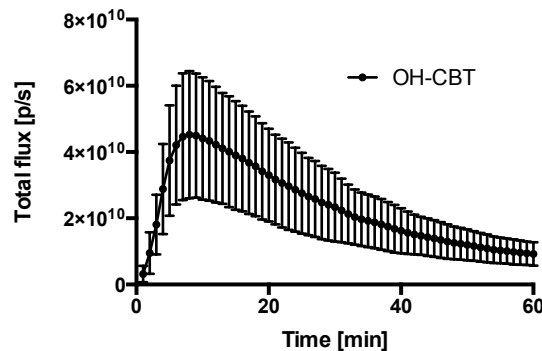


Figure 3-16 Kinetics of light emission for intraperitoneal injection of OH-CBT *in vivo*. Error bars are \pm SD for 4 measurements.

The kinetics of light emission *in vivo* after intraperitoneal injection of OH-CBT and D-cysteine is shown in Figure 3-16. Two mice presented a much lower light emission (Mice 12 and 51, see supplementary figure in the Annex) and were excluded to produce this graph. A strong peak is observed after 10 minutes of imaging followed by a gradual decrease in bioluminescence over the timecourse of the experiment.

3.3.4 CBT probes

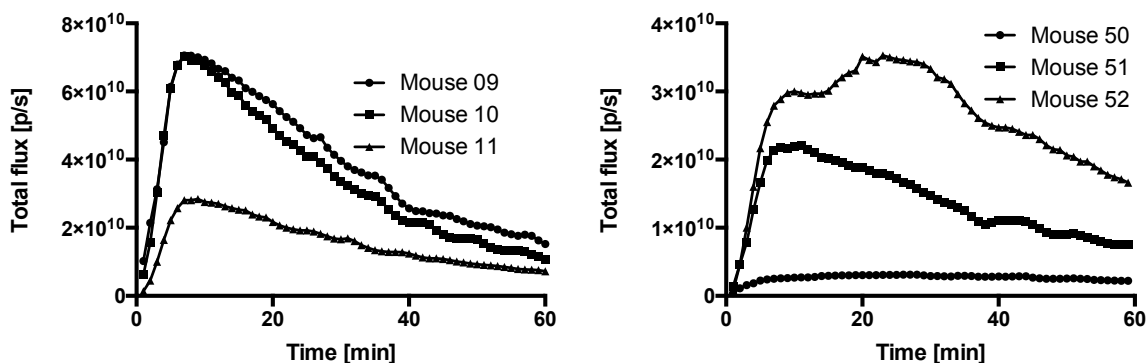


Figure 3-17 Kinetics of light emission for i.p. injection of C5-CBT (left) and C9-CBT (right) *in vivo*

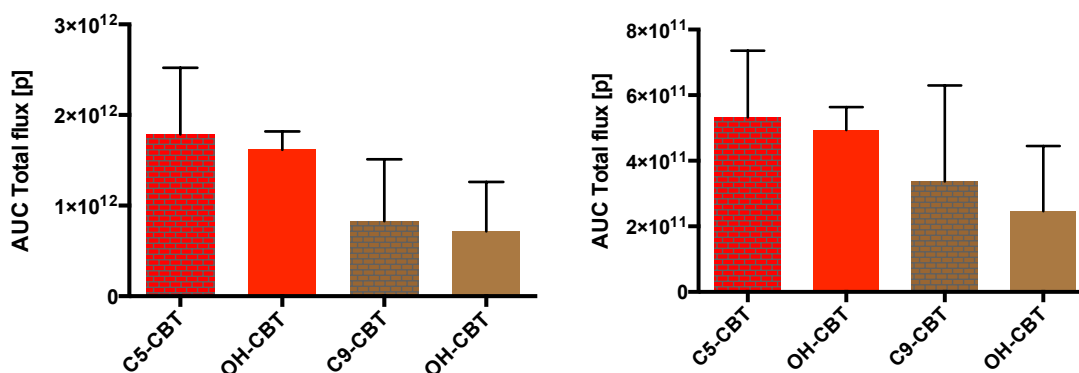


Figure 3-18 Total luminescence for CBT probes *in vivo* (left: 60 minutes integration, right: minute 30 to 60 integration). Error bars are \pm SD for 3 measurements.

The kinetics of light emission *in vivo* after intraperitoneal injection of C5-CBT and C9-CBT is presented in Figure 3-17. There is a peak in light emission at 10 minutes for C5-CBT and C9-CBT, but a second higher peak occurred for mouse 52 after 20 minutes. The decrease in light emission appears slower for C5-CBT and C9-CBT. The integration over the whole experiment shows a similar light emission for probes and OH-CBT. The signal is also similar for OH-CBT, C5 and C9 probes if we consider the last 30 minutes of imaging only (Figure 3-18).

3.3.5 Brain bioluminescence after intraperitoneal injection

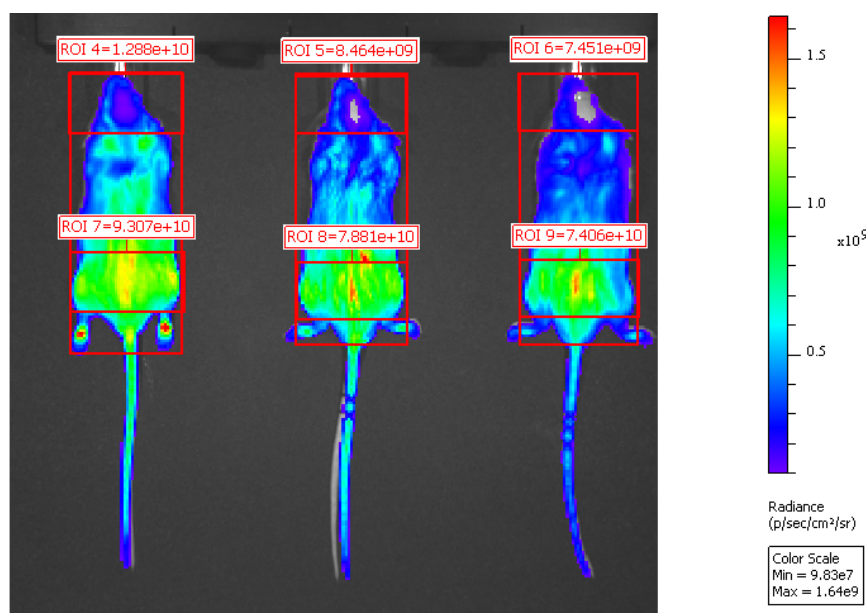


Figure 3-19 Definition of regions of interest (ROI) for the whole mouse, the head and the belly

In order to identify contribution of the head region in comparison to other parts of the body, a rectangular region of interest encompassing the whole mouse was defined and a smaller rectangle was used placed either on the head or belly part of the mouse. The disposition of these regions of interest is shown in Figure 3-19 Definition of regions of interest (ROI) for the whole mouse, the head and the belly

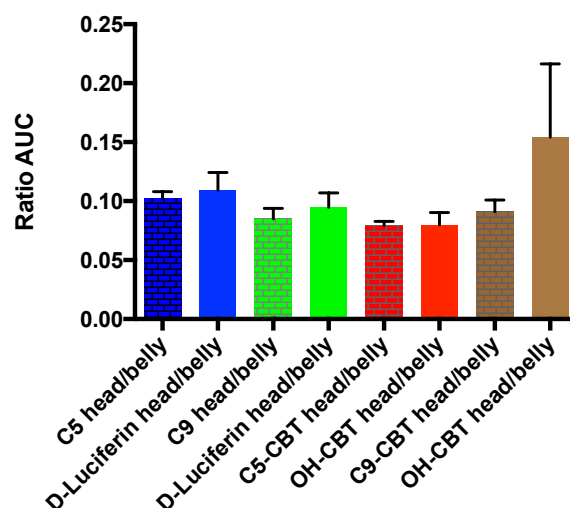


Figure 3-20 Ratios of contributions of head and belly ROIs to measured luminescence. Error bars are \pm SD for 3 measurements.

The relative contributions of the head and belly parts to the measured luminescence are presented in Figure 3-20. Statistical analysis were performed using an unpaired two-tailed Student's t-test to evaluate difference between alkylated derivatives and their respective controls. The ratio of the luminescence for the head and for the belly parts was calculated, and the ratio observed using our C5 or C9 Luciferin probes is not significantly different from D-Luciferin. No significant difference was observed between C5-CBT and OH-CBT. The head to belly ratio was higher for OH-CBT compared to C9-CBT, but this difference is mainly due to mouse 51 for which the ratio is abnormally bigger (see supplementary figure in the Annex).

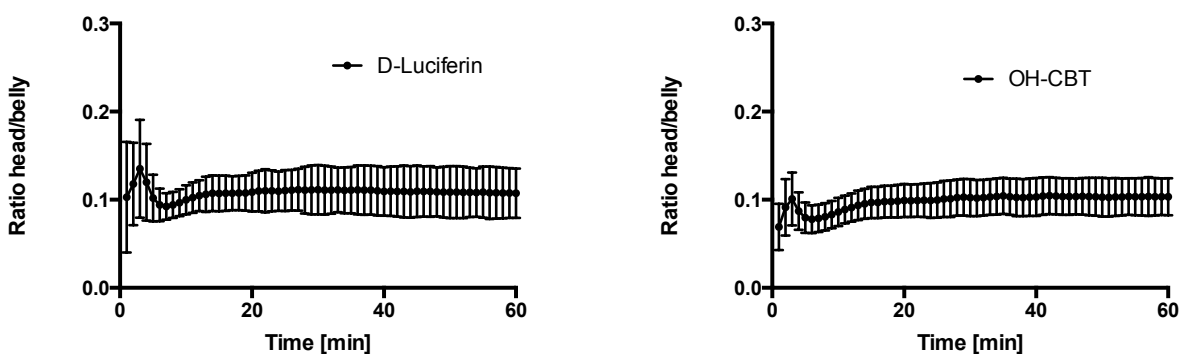


Figure 3-21 Evolution of the ROIs head to belly ratio for controls. Error bars are \pm SD for 4 measurements.

The evolution of the head to belly ratio during the *in vivo* bioluminescence imaging for D-Luciferin and OH-CBT controls is presented in Figure 3-21. A peak in the head to belly ratio is observed after 3 minutes, after which the ratio stabilizes to a value of 0,1.

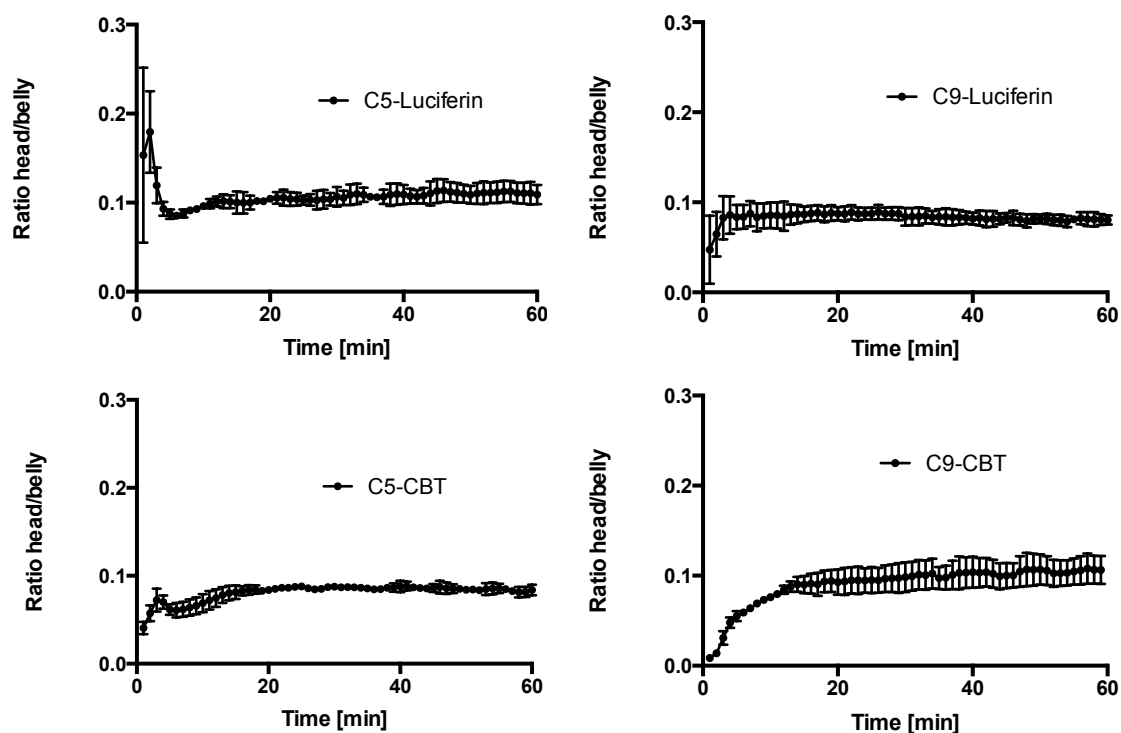


Figure 3-22 Evolution of the ROIs head to belly ratio for probes. Error bars are \pm SD for 3 measurements.

The evolution of the head to belly ratio during the *in vivo* bioluminescence imaging for our probes is presented in Figure 3-22. A peak in the head to belly ratio is observed after 2 minutes for the C5-Luciferin probe, and reaches a higher value than D-luciferin. The peak was not present for the other Luciferin or CBT derivatives for which a slower rise in the ratio was observed. The head to belly ratio was stable after a few minutes for all the probes. C9-Luciferin and C5-CBT displayed a smaller ratio compared to controls and other probes.

3.3.6 Brain bioluminescence after tail vein injection

To further evaluate the potential of our compounds for *in vivo* application, a formulation suitable for tail vein intravenous injection was obtained for the luciferin derivatives (see Section 1.2 in the Annex). A solution of D-Luciferin, OH-CBT, or their alkylated derivatives was prepared by dissolving the probe in a solution containing 0,5% DMSO in PEG:PG:PBS 1:1:2 and 200 μL of this solution were injected intravenously in the tail vein of luciferase expressing mice. Right after the injections, mice were anaesthetized and placed in the IVIS Specturm imaging chamber under isoflurane anaesthesia. Mice were imaged for 1h with 1 image per minute using the automatic settings.

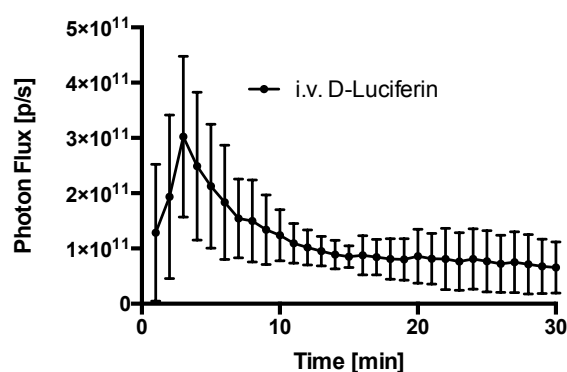


Figure 3-23 Kinetics of light emission for tail vein injection of D-Luciferin *in vivo*. Error bars are \pm SD for 3 measurements.

The kinetics of light emission *in vivo* after tail vein injection of D-Luciferin is presented in Figure 3-23. A peak in measured bioluminescence is observed after 3 minutes, followed by a decrease in signal with a stabilisation after 15 minutes.

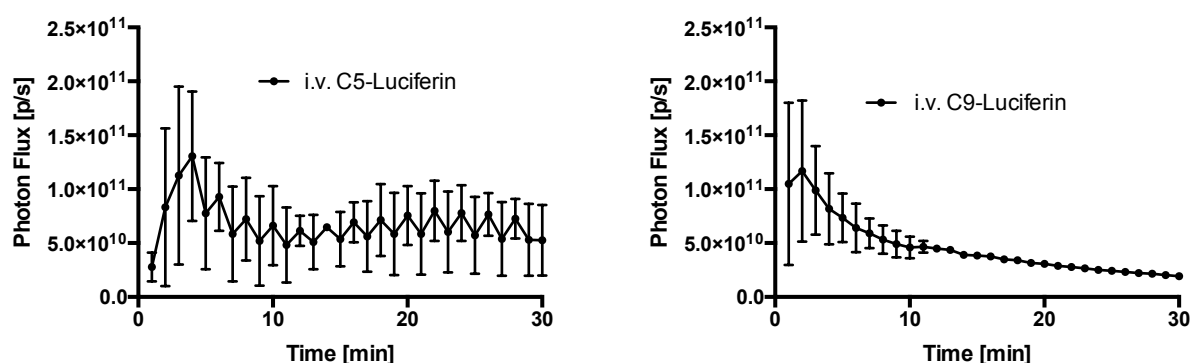


Figure 3-24 Kinetics of light emission for tail vein injection of C5-Luciferin and C9-Luciferin *in vivo*. Error bars are \pm SD for 3 measurements.

The kinetics of light emission *in vivo* after tail vein injection of C5-Luciferin and C9-Luciferin is presented in Figure 3-24. A peak in bioluminescence is observed after 4 minutes for C5-Luciferin and after 2 minutes for C9-Luciferin. A stable signal is observed for C5-Luciferin after 10 minutes. A slow decrease in signal is observed for C9-Luciferin over the time-course of the experiment.

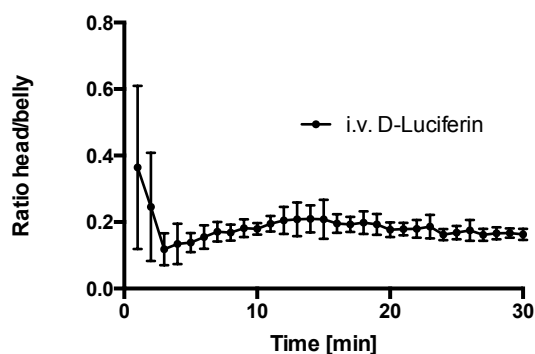


Figure 3-25 Evolution of the ROIs head to belly ratio for i.v. D-Luciferin. Error bars are \pm SD for 3 measurements.

The evolution of the head to belly ratio during the *in vivo* bioluminescence imaging for D-Luciferin after tail vein injection is presented in Figure 3-25. A peak in the head to belly ratio at 0,36 is observed after 1 minute, after which the ratio stabilizes to a value of 0,2.

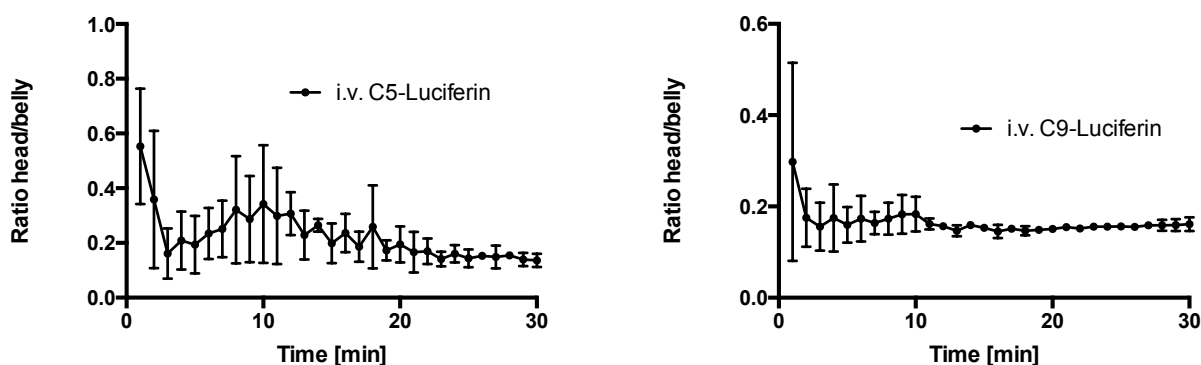


Figure 3-26 Evolution of the ROIs head to belly ratio for i.v. C5-Luciferin and C9-Luciferin. Error bars are \pm SD for 3 measurements.

The evolution of the head to belly ratio during the *in vivo* bioluminescence imaging for C5-Luciferin and C9-Luciferin after tail vein injection is presented in Figure 3-25. A peak in the head to belly ratio is observed after 1 minute, after which the ratio stabilizes to a value of 0,2. The maximum peak value is observed for C5-Luciferin with a value of 0,55. A higher ratio is also observed for C5-Luciferin after 10 minutes of imaging where it is around 0,3.

	Peak time [min]	Peak intensity [p/s]	30' intensity [p/s]	60' intensity [p/s]
D-Luciferin i.p.	8	$5.5 \cdot 10^{11}$	$1.78 \cdot 10^{11}$	$4.29 \cdot 10^{10}$
C5-Luciferin i.p.	13	$2.56 \cdot 10^{11}$	$1.65 \cdot 10^{11}$	$5.58 \cdot 10^{10}$
C9-Luciferin i.p.	18	$1.77 \cdot 10^{11}$	$1.49 \cdot 10^{11}$	$6.4 \cdot 10^{10}$
OH-CBT + D-Cys i.p.	8	$4.53 \cdot 10^{10}$	$2.34 \cdot 10^{10}$	$9.24 \cdot 10^9$
C5-CBT + D-Cys i.p.	7	$5.63 \cdot 10^{10}$	$2.99 \cdot 10^{10}$	$1.11 \cdot 10^{10}$
C9-CBT + D-Cys i.p.	20	$1.9 \cdot 10^{10}$	$1.7 \cdot 10^{10}$	$8.78 \cdot 10^9$
D-Luciferin i.v.	3	$3.02 \cdot 10^{11}$	$6.57 \cdot 10^{10}$	-
C5-Luciferin i.v.	4	$1.31 \cdot 10^{11}$	$5.27 \cdot 10^{10}$	-
C9-Luciferin i.v.	2	$1.17 \cdot 10^{11}$	$1.94 \cdot 10^{10}$	-

Table 3-1 Comparison of the light emission for D-Luciferin, OH-CBT and their derivatives *in vivo*

A comparison of the kinetics of the *in vivo* bioluminescence observed after intraperitoneal or intravenous injection of the probes is presented in Table 3-1. We observe slower kinetics for the alkylated luciferins injected intraperitoneally compared to D-Luciferin, but no noticeable difference is observed after tail vein injection. The kinetics observed for C5-CBT is similar to OH-CBT, with a higher signal observed at the different timepoints. A slower kinetics and less intense signal is observed for the C9-CBT derivative.

Chapter 4 Discussion

4.1 Synthesis

The synthesis of the alkylated derivatives of hydroxy-CBT by esterification with the activated fatty acids valeroyl chloride and nonanoyl chloride produced C5-CBT and C9-CBT with satisfactory yield, 84% and 51% respectively. The lower yield observed for the C9-CBT synthesis is explained by the second additional purification that was performed on a silica column, whereas only one purification was required for the C5-CBT. The condensation reaction between the alkylated CBTs and D-cysteine produced the corresponding C5-Luciferin and C9-Luciferin with a high yield after extraction, 83% and 90% respectively. The condensation reaction between the alkylated CBTs and the methyl ester of D-cysteine produced the corresponding C5-Luciferin methyl ester and C9-Luciferin methyl ester, but some unreacted alkylated CBT precursor could not be separated by extraction. We did not perform purification on a silica column because previous experiments performed in the lab showed that the majority of the product was degraded on silica. It was not possible to obtain a sufficient quantity of the alkylated Luciferins methyl esters with satisfactory purity. One of the issues encountered in this synthesis was the use of the hydrochloride salt of the D-cysteine methyl ester, which rendered the pH adjustment of the reaction difficult, as when the pH was too low ($\text{pH} < 7$), the reaction would not occur, and when the pH was too high ($\text{pH} > 8$), degradation of the reactant and the products would occur. One possible strategy to remove the unreacted alkylated CBT from the final product would be to react the obtained mixture again with D-cysteine and obtain a mixture of the alkylated Luciferin and the alkylated Luciferin methyl ester, which might be more easily separated by extraction or with column purification.

4.2 Test tube experiments

Previous studies have shown that firefly luciferase can accommodate changes in the D-Luciferin structure, notably in the substituting group on position 6 of the cyanobenzothiazole ring(8,9). The low light emission observed for our alkylated compounds suggest that either they are not good substrates for their oxidation by luciferase, or that the quantum yield of the oxidated state is lower compared to D-Luciferin (Figure 3-4 and Figure 3-6, left panels). The presence of a cell lysate clearly demonstrates an increase in the observed bioluminescence with time (Figure 3-3 to Figure 3-6), and we conclude that the addition of the cell lysate participates in the hydrolysis of the ester bond to release D-Luciferin. The increase in signal is even greater if we consider the expected decrease in signal upon addition of the cell lysate that is observed for the controls (Figure 3-2). We hypothesize that esterases or similar enzymes are present and responsible for the cleavage of the fatty acid chain from our alkylated compounds. Once the D-Luciferin is released, it can undergo the standard bioluminescence reaction by being enzymatically oxidated by luciferase and emitting a photon before returning to its ground state (Figure 1-1 and Figure 1-3).

The C9-Luciferins and C9-CBTs present a higher bioluminescence signal in comparison to the C5 derivatives and this could be explained by a faster rate of hydrolysis for the longer nine-carbon chain compared to the five carbon chain ester (Figure 3-4 and Figure 3-6).

The CBT derivatives seem to display a stronger signal compared to the D-Luciferin derivatives, but this effect is already present if we compare OH-CBT to D-Luciferin. Indeed, the signal displayed by OH-CBT combined with D-cysteine is higher than the already formed D-Luciferin (Figure 3-2). This superior signal for the split luciferin compared to the D-Luciferin itself was already shown to occur *in vitro*(4). A similar observation in test tubes is made here and might result from an autoinhibition of the D-Luciferin oxydation when it is present in high amounts, which would not take place if the D-Luciferin has to be formed from OH-CBT and D-cysteine in the tubes.

The effect of the methyl ester presence on the observed signal is more difficult to interpret since contradictory effects are observed. We should note that the D-cysteine methyl ester used was in the hydrochloride salt form and that a change in pH in the corresponding experiments might have influenced the observed bioluminescence. Indeed, a lowered pH due to the addition of the hydrochloride salt could favour the hydrolysis of the C5-CBT and C9-CBT to OH-CBT, resulting in the higher signal observed for these compounds when the methyl ester of D-cysteine was added in the experiment compared to the signal when the simple D-cysteine was added (Figure 3-4 and Figure 3-6). Regarding the luciferins methyl ester derivatives, we observe an improvement of the signal when the methyl ester is added to the C5-luciferin, but not when added to C9-Luciferin. The very high lipophilicity of the C9-luciferin resulted in a more difficult solubilisation, and it is possible that a fraction of the compound was not in solution.

We conclude from these test tubes experiments that our D-Luciferin and OH-CBT alkylated derivatives are not good substrates for luciferase. Then, hydrolysis of the ester bond can release the D-Luciferin or OH-CBT and result in light emission. From this observation, we propose that our compounds act as caged D-Luciferin or caged OH-CBT, similar to the principle which was previously developed in the lab for the bioluminescent imaging of capsase activity(4), hydrogen peroxide production (10) or fatty acid uptake (11). However, it is the activity of an esterase that is required for the hydrolysis of the ester bond to give D-Luciferin or OH-CBT, instead of relying on a protease activity or other biological processes to release D-Luciferin or OH-CBT from a caged probe. The ubiquitous distribution of esterases in cells of most tissues(12) lets us conclude that our compounds can be used both *in vitro* and *in vivo*, as their hydrolysis to release D-Luciferin or OH-CBT will be warranted once they have entered cells.

4.3 *In vitro* experiments

The potential of our D-Luciferin and OH-CBT derivatives was assessed by using a 4T1 luciferase expressing cell line and by recording the bioluminescence signal with an IVIS spectrum camera (PerkinElmer). We note again the superiority of the OH-CBT combined with D-cysteine over the preformed D-Luciferin for the *in vitro* bioluminescence (Figure 3-8). This observation might be accentuated in our experiment by the fact that the peak in bioluminescence that occurs for D-Luciferin is not recorded, possibly because it is occurring too early after addition of the D-Luciferin to the cell-containing wells (Figure 3-7). This could lead to an underestimation of the measured D-Luciferin bioluminescence signal.

The measured bioluminescence signal was superior for all our D-Luciferin derivatives compared to D-Luciferin itself (Figure 3-8, Figure 3-10 and Figure 3-12). We note the following progression in increasing observed bioluminescence signal from C9-Luciferin methyl ester, to C9-Luciferin, followed by C5-Luciferin methyl ester, and finally C5-Luciferin. The observed signal for C5-Luciferin integrated on the first 30 minutes of the experiments is one order of magnitude bigger than the signal observed for D-Luciferin. As D-Luciferin is the only luminogenic substrate released upon hydrolysis of the ester bonds of our alkylated D-Luciferin probes, this increase in signal must arise from their increased bioavailability. Their higher lipophilicity can explain this increased bioavailability by an improvement in the facilitated diffusion across the cell membrane. However, we note that C5-Luciferin, which provides the highest signal, is the least lipophilic

of our derivatives. A possible explanation is that the more lipophilic compounds might get trapped in the membrane, as an optimal partition coefficient is required for an efficient passive diffusion across membranes(7). Also, the methyl ester compounds give a lower signal compared to the compounds where the carboxylic acid is available, although this could simply be explained by the need for an additional hydrolysis, thus affecting the rate of release of the corresponding luciferin. The luciferin derivatives with a free carboxylic acid on one end and an aliphatic chain on the other end closely resemble the lipid bilayer components as amphipathic molecules, which could explain their facilitated passive diffusion. Another possible explanation for the observed signal increase for our probes is a different transport and efflux across the cell membrane. The involvement of a membrane transporter cannot be assessed from our experiment, but it is conceivable that our compounds, or some of them, use a facilitated or active transport across the cell membranes owing to their different structure. The efflux of the probes might also be influenced by their modification, changing their affinity for P-glycoprotein or other transporters of the ATP-binding cassette family, which are present in the 4T1 breast cancer cell line we used (13). Another interesting observation is made in the kinetics of light emission for our probes. After more than 45 minutes of imaging, there is still a very high and stable bioluminescence signal (Figure 3-9 and Figure 3-11, right panels). This observation is probably resulting from the time necessary for the probes to enter the cells, for the hydrolysis of the ester bond and release of D-Luciferin to occur, and finally for the oxidation of D-Luciferin by luciferase and the subsequent light emission. The combination of the different kinetics of these processes lead to the apparent steady state observed in our experiment. Such a high and stable signal after several minutes of imaging might be very useful to study longer events than what is possible to do with D-Luciferin. OH-CBT combined with D-Cysteine already acts as a slow-release luciferin (4) and other strategies have been developed like PEG-Luciferin to provide a longer imaging time *in vivo*, but no data is available for the bioluminescence obtained in cells (14).

For the OH-CBT derivatives, an improvement in light emission is also observed, except for C9-CBT that displays a lower bioluminescence than OH-CBT when combined with D-Cysteine (Figure 3-10 and Figure 3-12). We note an important signal reduction when using the methyl ester of D-Cysteine. As the hydrochloride salt of this reagent was used, there might be a negative influence on the cell function by the induced lower pH in the corresponding wells. Again, there appears to be an optimum in the lipophilicity of our compounds, as the C5-CBT displays a higher signal than C9-CBT. The latter was the most hydrophobic compound and it was even difficult to solubilize it for the *in vitro* experiments, where relatively low concentrations of the probes were used (100 μ M). The signal obtained with C5-CBT and D-Cysteine integrated over 30 minutes is 2,34 times higher than the signal obtained for OH-CBT and D-Cysteine, and 14,84 times higher than D-Luciferin. The complete process for bioluminescence with these novel OH-CBT derivatives needs the alkylated OH-CBT and D-Cysteine to enter the cell, the hydrolysis of the ester bond to release OH-CBT, the click reaction between OH-CBT and D-Cysteine to form D-Luciferin, and the bioluminescence reaction with its oxidation by luciferase (Figure 1-1 to Figure 1-3). These processes probably account for the different kinetics observed for these compounds. Indeed, their light emission is low in the beginning but rises rapidly to levels above those of the D-Luciferin derivatives to reach a stable light emission (Figure 3-9 and Figure 3-11). Thus, in addition to the higher signal obtained, we observe again a strong and stable bioluminescence after a longer imaging time. These experiences confirm the prolonged imaging potential of our probes, not only as extended release D-Luciferin, but also as extended release OH-CBT.

4.4 Formulation for *in vivo* experiments

The formulation of compounds for the *in vivo* experiments is important in order to avoid deleterious effect for the imaged animals. Such effort is a considerable part of preclinical studies, especially for compounds with high lipophilicity(15). Indeed, lipophilic compounds are more difficult to solubilize in commonly used formulations and solubility problems might result in the formation of thrombus if injected in an animal. Two routes of administration of the compounds were considered in this project, intraperitoneal injection and intravenous injection in the tail vein of the mouse. As a comparison between the different synthesized derivatives is desired, we tried to obtain a formulation for the most lipophilic compounds, C9-CBT. Unfortunately, it was not possible to obtain an intravenous-compatible formulation for this compound. The only vehicle in which C9-CBT was soluble at desired concentration was PEG400, but it was not possible to mix it with PBS to reach adequate PEG400 volume and percentage for intravenous injection, even with the help of a surfactant like Tween20 (see Annex). It was not possible to use BSA in PBS (see Annex) as was previously used for the formulation of a free fatty acid caged D-Luciferin(11). This is probably due to the fact that the carboxylic acid of the fatty acid must be available for suitable binding to BSA. Thus, a formulation for the intraperitoneal injection was investigated as less stringent conditions can be used for this route of administration. As it was not possible to find any suitable aqueous formulation, we decided to solubilize the compounds in a small volume of DMSO that can be tolerated by the animals (see Annex). As the lipophilicity of the D-Luciferin derivatives is not as important as for the OH-CBT derivatives, a formulation for the intravenous injection of the C5-Luciferin and C9-Luciferin was investigated. Again, the formulation using BSA in PBS was not suitable as we noted the formation of a precipitate. It was possible to solubilize the C9-Luciferin in a small volume of DMSO, further mixed with PEG:PG 1:1 and PBS. The final volume of PEG:PG in the formulation is 100 μ L mixed with 100 μ L PBS, and the percentage of DMSO is only 0,5% (see Annex), making it suitable for *in vivo* bioluminescence imaging with intravenous administration of our probes.

4.5 *In vivo* experiments

The bioluminescence signal obtained after intraperitoneal injection of D-Luciferin and OH-CBT was in agreement with previous experiments performed in the group(4). Some mice displayed a reduced signal, which is most likely due to injection of the compounds in the bowel loops(1), and the mice with a very low signal were not included in the analysis. The signal displayed by our probes is similar in intensity to their respective controls D-Luciferin and OH-CBT, if integrated over the whole experiment (Total luminescence for luciferin probes *in vivo* (left: 60 minutes integration, right minute 30 to 60 integration)). The kinetics of light emission differed slightly, as the peak in bioluminescence was delayed and smaller in intensity, but the remaining light emission at the end of the experiment was higher for our probes (Table 3-1). After intraperitoneal injection, it is possible that the alkylated probes are rapidly hydrolysed and that they effectively reach the bloodstream as their D-Luciferin or OH-CBT counterpart, especially if they pass through the liver as it contains a high amount of esterases and other biotransforming enzymes(16). Also, esterases and hydrolases present in the blood might reduce the stability of the alkylated probes. It would be interesting to test the rate of hydrolysis of our probes in blood to account for this possibility. Thus, the different longer kinetics observed for our probes could result from the time needed to hydrolyse the ester bond before reaching the target cells. Nevertheless, it is possible that a fraction of the probes reaches the bloodstream and organs of the mice unaltered before being hydrolysed by cytosolic enzymes.

As the mouse model used express luciferase in a ubiquitous fashion, it is difficult to isolate the bioluminescence signal resulting from brain cells. In order to compare between the different compounds, regions of interest (ROI) of identical dimensions were defined on the head and on the belly of the mice (Figure 3-19). No clear advantage was observed for our probes in the ratio of head to belly bioluminescence. It is interesting to note that the signal from the head region is 10-fold lower than the signal emanating from the belly, and that this ratio is similar for all the tested compounds (Figure 3-20). However, notable differences can be found in the first minutes of the experiments. Indeed, the C9-Luciferin and alkylated CBTs show a slow rise in the ratio, indicating that the probes take a long time to reach the head region. A higher peak in the ratio is observed for C5-Luciferin is observed in the first minutes, even higher than the peak observed for D-Luciferin and OH-CBT (Figure 3-21 and Figure 3-22). The higher lipophilicity of the alkylated CBTs and C9-Luciferin might result in a slow diffusion from the point of injection and thus higher signal from the belly region as the probes were injected intraperitoneally. It is not possible to conclude from the exact origin of the signal emanating from the head region, but the higher peak in head to belly bioluminescence ratio for C5-Luciferin might indicate that a higher portion of the probe reaches the brain. It would be interesting to have a model with mice that express luciferase in the brain only in order to confirm this possibility.

As a high proportion of the alkylated probes might be hydrolysed after passage in the liver, the intravenous route of administration was tested in order to better reach the brain. The signal obtained for the alkylated derivatives C5 and C9-Luciferin was almost identical to the signal obtained with D-Luciferin, although the peak in bioluminescence signal was brighter for D-Luciferin (Figure 3-23 and Figure 3-24). There is a higher head to belly ratio after tail vein injection compared to intraperitoneal injection, indicating that a higher proportion of the probes reach the head region. There is no significant advantage for the alkylated luciferins to reach the brain, although the ratio after 10 minutes of experience seems to be higher for C5-Luciferin. Again, a model where the mouse express luciferase in the brain only is needed to assess for the potential central nervous system origin of the signal, as this higher ratio might simply represent a better distribution of the bioluminescent probe in the whole animal.

Chapter 5 Conclusion

A family of alkylated D-Luciferin and OH-CBT derivatives has been prepared during this work with the goal of making these bioluminescent substrates more lipophilic, facilitating their passage across cell membranes through passive diffusion, with the final objective of improving the bioluminescent signal obtained from the central nervous system. OH-CBT has been reacted with valeroyl and nonanoyl chloride to form the corresponding esters C5-CBT and C9-CBT. After condensation with D-Cysteine, the resulting C5-Luciferin and C9-Luciferin have been obtained. The methyl esters of alkylated luciferins were synthesized, but some unreacted CBT precursor could not be separated from the product to yield C5-Luciferin methyl ester and C9-Luciferin methyl ester with satisfactory purity for *in vivo* injection.

The bioluminescence obtained with these alkylated derivatives was measured in solution in presence of luciferase and the signal was low, indicating a low efficiency in the substrate binding to luciferase, or a lower rate of substrate oxidation. Upon addition of a cell lysate in the test tubes, a gradual increase in signal is observed. This suggests that enzymes present in the lysate hydrolyse the ester bond of the alkylated derivatives, allowing for the release of the corresponding D-Luciferin or OH-CBT and light emission after reaction with luciferase.

A strong signal was obtained *in vitro* after addition of the alkylated derivatives to 4T1 cells expressing luciferase. The signal was higher for the lipophilic probes compared to their D-Luciferin or OH-CBT equivalent, and the kinetics observed showed a longer lasting signal, with a strong bioluminescence signal even after one hour of experiment. This improved signal is likely due to the possibility for alkylated bioluminescent probes to cross the cell membranes more efficiently and to be hydrolysed once inside the cytosol to release the corresponding D-Luciferin or OH-CBT.

The signal obtained *in vivo* in mice expressing luciferase (FVBLuc+; FVBTg/CAG-luc, -GFP)L2G85Chco/J) after intraperitoneal injection of the alkylated derivatives showed a bioluminescent signal comparable to the signal obtained with their D-Luciferin or OH-CBT counterpart. In order to evaluate the potential to target the brain, a ratio of the contribution to the bioluminescent signal from the head or the belly region was measured and was consistently around 0.1 for the different compounds injected. No significant advantage was observed for the alkylated derivatives, although the ratio observed for C5-Luciferin in the first minutes after injection was the highest observed.

After tail vein injection of D-Luciferin, C5-Luciferin and C9-Luciferin, we observed a bioluminescence signal with faster kinetics compared to the intraperitoneal injection. The signal obtained with the alkylated luciferins was comparable to D-Luciferin, although the intensity of the light emission was slightly lower. The ratio of the head to belly contributions to the bioluminescent signal was consistently measured around 0.2

after tail vein injection, indicating a better distribution of the bioluminescent probes across the animal compared to the intraperitoneal injection route of administration. Again the ratio observed for C5-Luciferin after 10 minutes was the highest observed, but no significant advantage could be demonstrated in the bioluminescence obtained from the brain.

The future objectives of this project are to improve the synthesis of the methyl esters of the alkylated luciferins, in order to obtain compounds of sufficient purity and quantity for *in vivo* experiments. The different alkylated compounds should be used for the *in vitro* imaging in different cell lines to better characterise their *in vitro* light emission and to assess that the strong signal that was observed in 4T1 cells was not specific to this particular cell line. The stability of the probes in the blood or serum should also be assessed in further experiments to investigate a possible hydrolysis by enzymes present therein. A measure of the hydrolysis rate using purified esterases enzymes at various concentrations could be performed in order to assess for the role of esterases in the rate of release of the D-Luciferin or OH-CBT from the caged probes. A negative control for the *in vitro* or *in vivo* experiments could be performed by treating the cells or animals with esterases inhibitors. In order to better assess the propensity of the different bioluminescent probes to reach the central nervous system and brain parenchyma, it would be preferable to find an animal model where the luciferase is conditionally expressed in brain cells only, in order to compare the obtained signal among different probes with higher specificity. One further avenue for the improvement in the bioluminescent signal obtained from the brain is to attach other molecules to use other mechanisms of transport across the blood-brain barrier, like active transport. Such molecules could be attached covalently to D-Luciferin or OH-CBT and release the bioluminescent substrate once they have reached the brain. Different molecules like glucose, neurotransmitters or analogues, neuropeptides, proteins like transferrin or carriers such as nanoparticles could be envisioned.

References

1. Close DM, Xu T, Saylor GS, Ripp S. In Vivo Bioluminescent Imaging (BLI): Noninvasive Visualization and Interrogation of Biological Processes in Living Animals. *Sensors*. 2011 Jan;11(1):180–206.
2. Sletten EM, Bertozzi CR. Bioorthogonal Chemistry: Fishing for Selectivity in a Sea of Functionality. *Angew Chem Int Ed*. WILEY-VCH Verlag; 2009 Sep 7;48(38):6974–98.
3. Niwa K, Nakamura M, Ohmiya Y. Stereoisomeric bio-inversion key to biosynthesis of firefly d-luciferin. *FEBS Letters*. 2006 Sep 11;580(22):5283–7.
4. Godinat A, Park HM, Miller SC, Cheng K, Hanahan D, Sanman LE, et al. A biocompatible in vivo ligation reaction and its application for noninvasive bioluminescent imaging of protease activity in living mice. *ACS Chem Biol*. 2013 May 17;8(5):987–99.
5. Hochgräfe K, Mandelkow E-M. Making the Brain Glow: In Vivo Bioluminescence Imaging to Study Neurodegeneration. *Mol Neurobiol*. Humana Press Inc; 2012 Nov 29;47(3):868–82.
6. Evans MS, Chaurette JP, Adams ST, Reddy GR, Paley MA, Aronin N, et al. a synthetic luciferin improves bioluminescence imaging in live mice. *Nature Methods*. Nature Publishing Group; 2014 Feb 9;:1–4.
7. Liu X, Testa B, Fahr A. Lipophilicity and Its Relationship with Passive Drug Permeation. *Pharm Res*. Springer US; 2010 Oct 30;28(5):962–77.
8. Adams ST Jr, Miller SC. ScienceDirectBeyond D-luciferin: expanding the scope of bioluminescence imaging in vivo. *Current Opinion in Chemical Biology*. Elsevier Ltd; 2014 Aug 1;21:112–20.
9. Iwano S, Obata R, Miura C, Kiyama M, Hama K, Nakamura M, et al. Development of simple firefly luciferin analogs emitting blue, green, red, and near-infrared biological window light. *Tetrahedron*. Elsevier Ltd; 2013 May 13;69(19):3847–56.
10. Van de Bittner GC, Dubikovskaya EA. In vivo imaging of hydrogen peroxide production in a murine tumor model with a chemoselective bioluminescent reporter. 2010.
11. Henkin AH, Cohen AS, Dubikovskaya EA, Park HM, Nikitin GF, Auzias MG, et al. Real-time noninvasive imaging of fatty acid uptake in vivo. *ACS Chem Biol*. 2012 Nov 16;7(11):1884–91.
12. Gilham D, Lehner R. Techniques to measure lipase and esterase activity in vitro. *Methods*. 2005 Jun;36(2):139–47.
13. Zhao L, Jin X, Xu Y, Guo Y, Liang R, Guo Z, et al. Functional study of the novel multidrug resistance gene HA117 and its comparison to multidrug resistance gene 1. *J Exp Clin Cancer Res*. BioMed Central; 2010;29(1):98–7.
14. Chandran SS, Williams SA, Denmeade SR. Extended-release PEG-luciferin allows for long-term imaging of firefly luciferase activity in vivo. *Luminescence*. John Wiley & Sons, Ltd; 2009 Jan;24(1):35–8.
15. Li P, Zhao L. Developing early formulations: Practice and perspective. *Int J Pharm*. 2007 Aug;341(1-2):1–19.
16. Polsky-Fisher SL. EFFECT OF CYTOCHROMES P450 CHEMICAL INHIBITORS AND MONOCLONAL ANTIBODIES ON HUMAN LIVER MICROSOMAL ESTERASE ACTIVITY. *Drug Metabolism and Disposition*. 2006 May 19;34(8):1361–6.